INSTITUTE OF PLASMA PHYSICS

NAGOYA UNIVERSITY

RESEARCH REPORT

NAGOYA, JAPAN

Free Boundary MHD Equilibria in Axisymmetric Tori

Y. Suzuki

IPPJ-180 December 1973

Further communication about this report is to be sent to the Research Information Center, Institute of Plasma Physics, Nagoya University, Nagoya, Japan.

Abstract

A method of numerical computation is presented to obtain the equilibrium configurations in axisymmetric tori with the ideally conductive shells of arbitrary cross-sections and/or with control field coils. In this method an artificial function $S(\psi)$ is introduced, which makes it possible to combine the equilibrium equations in the plasma and the equation for the vacuum into one equation. The alternating direction implicit method coupled with the Marder-Weitzner iteration scheme is used to solve the combined equilibrium equation under the boundary condition given on the shell. The continuity conditions at the plasma-vacuum interface are satisfied automatically in the obtained solutions. Some results of the computation are illustrated for cases where the shell shapes are circle, square, rectangle and finger ring type respectively and for a case with a ring coil placed inside the square shell.

I. Introduction

Recently there have been several new proposals of the advanced Tokomak-like devices with the non-circular plasma cross-section in order to raise the critical values of the toroidal current and/or poloidal beta; doublet [1], tear drop [2], belt pinch [3], ATC [4], finger ring [5] and multipole Tokomak [6].

For the design of such axisymmetric toroidal devices with the non-circular plasma cross-section or for the analysis of experimental data from such devices, theoretical estimates are necessary about the equilibrium position and the geometric shape of the plasma cross-section. The plasma characteristics (pressure distribution, current distribution and so on) and the environment around the plasma (the locations of control field coils, their field intensities, the shape of the conductive shell and so on) give effects on the plasma shape. In the usual treatment on MHD equilibrium of Tokomak with a shell of the circular cross-section the plasma cross-section is assumed to be also circular. And then, the general solutions of the fields in the plasma region and in the vacuum one are calculated separately and the obtained fields are connected each other on the plasma surface. This method is not convenient for the case of a shell of the non-circular cross= section, since it is not easy to assume the adequate shape of the plasma cross-section for this case. In the method

described in this paper the assumption about the shape of the plasma cross-section is not needed. It is determined from plasma parameters and the condition on the ideally conductive shell or at infinity. By introducing an artificial function $S(\psi)$ the equilibrium equation in the plasma and the equation for the vacuum field are combined into one equation. The combined equation is solved under the boundary condition on the shell, and the continuity conditions on the plasma surface are satisfied automatically. So, if only the boundary conditions on the shell or at infinity is given, the plasma shape is determined self-consistently.

In section II, the formulation of the equilibrium problem is written for a simple case in which the number of free parameters is restricted and the physical meanings of the parameters can be easily understood. The method to give the boundary condition for the various environment (shell shapes, control fields and so on) is also described.

In section III, results of computation are presented for the plasma equilibria in the shells of the various shapes; circular, square, belt pinch type, finger ring type.

The conclusion is presented in section IV. In Appendix the numerical method for solving the equilibrium problem is described and the condition for the convergence of the iteration scheme is discussed.

II. Formulation of the Equilibrium Problem

In the cylindrical coordinate system (R, ϕ, Z) ideal MHD equilibria with axial symmetry are described by solutions of the equation for the flux function ψ [7],

$$L\psi = -\frac{8\pi^2}{c}\left(2\pi cR^2 \frac{dp}{d\psi} + \frac{1}{c}\frac{dI^2}{d\psi}\right), \tag{1}$$

$$= -\frac{8\pi^2}{c} Rj_\phi,$$

where $L = R\frac{\partial}{\partial R}\frac{1}{R}\frac{\partial}{\partial R} + \frac{\partial^2}{\partial Z^2}$, and p and I, which are the pressure and the current stream function respectively, are functions of ψ only. The magnetic flux density and the current density are expressed by the following equations,

$$\vec{B} = (2I/cR)\vec{\phi} + \nabla\psi \times \vec{\phi}/2\pi R \tag{2}$$

and

$$\vec{j} = j_\phi\vec{\phi} + \nabla I \times \vec{\phi}/2\pi R. \tag{3}$$

In order to make the problem simple we consider the case where $p(\psi)$ and $I^2(\psi)$ are expressed by quadratic forms of ψ with constant coefficients respectively and the vacuum magnetic field containing the plasma is surrounded by a continuous ideally conductive shell. We can denote the plasma surface, where p = 0, by the surface of ψ = 0 without loss of generality. By imposing the restriction on the constant coefficients mentioned above that the toroidal

current j_ϕ vanishes on the plasma surface, Eq.(1) is re-written by

$$L\psi + (\lambda^2 R^2 + \mu)\psi = 0, \tag{4}$$

where $\lambda^2 = 32\pi^3 p_0/\psi_0^2$, $\mu = 16\pi^2(I_0^2 - I_s^2)/c^2\psi_0^2$ and sufixes 0 and s indicate the quantities on the magnetic axis and on the plasma boundary respectively [8, 9]. The functions $p(\psi)$ and $I^2(\psi)$ are expressed by

$$p(\psi) = \frac{\lambda^2}{32\pi^3}\psi^2, \tag{5}$$

and

$$I^2(\psi) = I_s^2 + \frac{c^2}{16\pi^2}\mu\psi^2. \tag{6}$$

From the above expressions it is induced that the pressure gradient and the poloidal current j_p vanish at the plasma boundary, since $(\partial p/\partial\psi)_{\psi=0} = 0$ and

$$|j_p|_{\psi=0} \propto I_s^{-1}|\nabla I^2|_{\psi=0} = 0.$$

In the vacuum region surrounding the plasma the flux function must satisfy the equation

$$L\psi = 0, \tag{7}$$

with the boundary condition on the shell surface and with the boundary conditions on the plasma surface that $\psi = 0$

and the first derivatives of ψ are continuous (note that $\vec{j} = 0$ on the plasma boundary).

Equations (4) and (7) can be combined into one equation,

$$L\psi + S(\psi)(\lambda^2 R^2 + \mu)\psi = 0, \tag{8}$$

by introducing a function $S(\psi)$ which is defined as follows,

$$S(\psi) = 1, \qquad \text{where } \psi \geqq 0 \tag{9}$$

$$S(\psi) = 0, \qquad \text{where } \psi < 0. \tag{10}$$

We assume here that $\psi \geqq 0$ in the plasma region and $\psi < 0$ in the vacuum region. When the external control fields are not applied, the boundary condition on the shell surface is

$$\psi = A \text{ (negative const.)} \tag{11}$$

from the condition that the normal component of magnetic field vanishes there. The constant A should be negative to ensure isolation of the plasma from the shell.

So the problem to treat with is to look for the continuous solution of Eq.(8), which satisfies the boundary condition (11) and has the continuous first derivatives.

We solve the differential equation (8) by a numerical method: equation (8) is written into the finite-difference equation and solved with the ADI method combined with

the Marder-Weitzner iteration scheme [10]. This numerical method (see Appendix) has been checked, for one dimensional case, by comparing the numerical solution of the following equation with its analytic solution,

$$\frac{d^2\psi(x)}{dx^2} + k^2\psi(x)S(\psi(x)) = 0, \tag{12}$$

the boundary conditions being $\psi = A$ at $x = x_1$ and x_2 and $d\psi/dx$ is continuous at the points of $\psi = 0$. The both solutions agree satisfactorily well and, of course, ψ and $d\psi/dx$ are continuous. For the two dimensional case we have compared the results obtained by the numerical method with the results obtained analytically from the formula developed for the ordinary Tokomak [7] with the circular plasma cross-section (see III. A)).

One of the features of the solutions of Eq.(8) with the boundary condition (11) is that the geometric shape of the plasma surface does not depend on the boundary value A. Because when αA is chosen as the boundary value, $\psi = \alpha\psi_A$ is the solution of Eq.(8), where ψ_A is the solution of Eq.(8) with the boundary condition (11). This fact means that the surface defined by $\psi = 0$ is invariant to the change of the boundary value. Here it is necessary to remark that, as the total toroidal plasma current J_ϕ is proportional to α and the mean pressure $\bar{P}$ to α^2, the ratio $\bar{P}/J_\phi^2$, which defines the poloidal beta, does not depend on

the boundary value also.

Another feature is that there are two solutions; one is a shallow solution [10], for example, ψ = A and the other is a deep solution. The former solution, however, is easily taken away by choosing a proper approximating function at the initial iteration step. The choice of the approximating function is not crucial.

Now, we consider the cases where the external axisymmetric field is applied in order to control the position or the shape of the plasma, for example, from the requirements for stability. We assume that the flux function for the external field is given by ψ_e which, for example, is expressed by cR^2, c being a constant, for the vertical uniform field or by the formula with the elliptic functions for the field produced by currents flowing in ring coils.

At first, we consider the case where the control coils are located outside the shell and the field is frozen in the shell. The equation for ψ is the same as Eq.(8), but the boundary condition becomes

$$\psi = A + \psi_{eb} \text{ on the shell surface,} \qquad (13)$$

where ψ_{eb} is the value of ψ_e on the shell surface. Why the boundary condition can be given by Eq.(13) is explained as follows. Denoting the flux functions in the shell by ψ_e and in the vacuum region near the shell by ψ_v, the continuity condition of the normal component of the magnetic

flux on the shell surface can be written by the following expression,

$$\frac{\partial(\psi_v, g)}{\partial(R,Z)} = \frac{\partial(\psi_e, g)}{\partial(R,Z)} , \tag{14}$$

where $\frac{\partial(\psi_v, g)}{\partial(R,Z)} = \frac{\partial\psi_v}{\partial R}\frac{\partial g}{\partial Z} - \frac{\partial g}{\partial R}\frac{\partial\psi_v}{\partial Z}$ and the shell surface is given by $g(R,Z) = 0$. Hence, $\psi_v - \psi_e$ is a function of $g(R,Z)$ or takes a constant value on the shell surface.

The same boundary condition can be applied to the case where the control coils (ring coils) are located inside the shell, as far as the field produced by them is steady one. However, as the currents in the coils have to be taken into account, the differential equation for ψ becomes

$$L\psi + S(\psi)\psi f(R) + \frac{8\pi^2}{c}\Sigma_i RJ_i\delta(R-R_i, Z-Z_i) = 0, \tag{15}$$

where $f(R) = \lambda^2R^2 + \mu$ and we have expressed the currents flowing in the ring coils by $J_i\delta(R-R_i, Z-Z_i)$ and the positions of the coils by (R_i, Z_i). If we put $\psi = \psi_e + \psi_p$ into Eq.(15) we have the following equation for ψ_p which is to be solved;

$$L\psi_p + S(\psi_p + \psi_e)\psi_p f(R) = -S(\psi_p + \psi_e)\psi_e f(R), \tag{16}$$

where we have used the relation,

$$L\psi_e + \frac{8\pi^2}{c}\Sigma_i RJ_i\delta(R-R_i, Z-Z_i) = 0. \tag{17}$$

The boundary condition for ψ_p becomes

$$\psi_p = A \text{ on the shell.} \tag{18}$$

When the control field is produced pulsively, the value of ψ on the shell surface becomes a constant. So the boundary condition for ψ_p becomes

$$\psi_p = A - \psi_{eb}. \tag{19}$$

In these three cases the shallow solution represents the vacuum field and especially for the last case it includes the effect of the image current induced in the shell.

There may be the cases where the value of ψ is positive in some regions where the plasma current should not flow, for instance in the neighborhood of the control coils. For these cases we introduce the 'virtual limiter' only inside which the plasma current can flow. The role of the 'virtual limiter' can be translated in the numerical computation as follows; the function $S(\psi)$ which is expressed in Eqs.(9) and (10) is modified into the function $S(\psi, R, Z)$. The definition of $S(\psi, R, Z)$ is

$S(\psi, R, Z) = 1$ in the regions of $\psi \geqq 0$ inside the limiter, (20)

and

$S(\psi, R, Z) = 0$ in the other regions. (21)

By choosing proper parameters λ^2, μ, A and J_i's we have solutions which represent the plasma localized inside the 'virtual limiter'.

Without the shell the equilibrium of the plasma is obtained by the control field. In such a case we introduce the 'virtual shell' which is placed far from the plasma so that the effect of the current induced in the shell on the plasma shape may be neglected. Because, the deformation of the plasma shape due to the presence of the external current-carrying conductors, in our case the shell, is determined by the ratio between the external field and the magnetic field produced by the plasma current at the plasma surface [11].

In the case of the open shell we introduce the 'virtual shell', which is placed far from the region occupied by the plasma, to make the shell close.

Thus, we can solve the MHD equilibrium equation for the various boundary conditions.

III. Solutions for Several Shell Cross-Sections

For the computation, the shape of the shell, an initial approximating function ψ_1 and parameters λ^2 and μ must be given. Another parameter I_s^2 must also be given to determine the vacuum toroidal field. When informations about the safety factor q are required, I_s^2 should be replaced by a

parameter M. The physical meanings of λ^2, μ and M can be understood from the following expressions, which are given in previous papers [8, 9],

$$\lambda^2 = \bar{\beta}_p/(R_0^2 - R_s^2)^2, \tag{22}$$

$$\mu = MQ^2R_0^4/(R_0^2 - R_s^2)^2(R_0 - R_s)^2, \tag{23}$$

and

$$M = (B_{\phi 0}^2/B_{\phi 0v}^2) - 1, \tag{24}$$

where R_0 and R_s are the radii of the position of the magnetic axis and the inner edge of the plasma respectively, $\bar{\beta}_p = 8\pi p_0/\bar{B}_Z^2$, $Q = (R_0 - R_s)B_{\phi 0v}/R_0\bar{B}_Z$, $\bar{B}_Z$ is the mean value of the poloidal field between the inner edge of the plasma and the magnetic axis in the median plane $Z = 0$, $B_{\phi 0v}$ is the vacuum toroidal field on the magnetic axis. Note that, although the parameters $\bar{\beta}_p$ and Q correspond to the poloidal beta β_p and the safety factor q respectively, in the definitions of the formers $\bar{B}_Z$ is used instead of the poloidal field on the plasma surface. Also note that plasma is paramagnetic (diamagnetic) when M is positive (negative). As is well known [8, 12], β_p and M are not independent each other ($M \simeq 0$ corresponds to $\beta_p \sim 1$ and $M < 0$ does to $\beta_p \gtrsim 1$). So, if we give rough estimations for β_p, q and geometric factors of the plasma surface, the values of parameters λ^2, μ and M to be given for the computation can be chosen by use of the relations (22)-(24). Several runs of the

calculation have shown a tendency that, when μ is small, λ^2 has an effect on the plasma size, μ/M on q value and M on β_p.

After the solution ψ is obtained, β_p and q are calculated from the following definitions,

$$\beta_p = \frac{8\pi \int p\,ds / \int ds}{\left(\int B_p\, d\ell / \int d\ell\right)^2}, \tag{25}$$

and

$$q = \frac{d\Phi}{d\psi}\Big|_{\psi=0}, \tag{26}$$

where $d\Phi$ means the toroidal magnetic flux between the neighboring magnetic surfaces ψ and $\psi + d\psi$. The total toroidal current is calculated from Eqs.(1), (5) and (6).

Now, we describe results of the computation for some cases where the shell shapes are circle, square, rectangle and finger ring type respectively. In all cases we have chosen the minimum radius of the shell R_{min} as 30 cm and the maximum R_{max} as 60 cm.

A) The Shell of Circular Cross-Section

Figure 1 shows an example of results of the computation for the case of the shell of the circular cross-section. The plasma surface is drawn by a bold line. The plasma surface is almost circular when $\beta_p \lesssim 1$ as many articles have reported [7, 12]. We have compared computational results with analytical results obtained from the relation between the geometrical characteristics and plasma parameters [7],

that is,

$$\Delta = \frac{b^2}{2R}\left\{\ell n\,\frac{b}{a} + \left(1 - \frac{a^2}{b^2}\right)\left(\beta_p + \frac{\ell_i}{2} - \frac{1}{2}\right)\right\} - \frac{B_0}{B_b}\,, \tag{27}$$

where the internal inductance ℓ_i of the plasma is defined by

$$\frac{1}{2C^2}\,\ell_i J_\phi^2\,\frac{V}{S} = \frac{1}{8\pi}\int B_p^2 dV, \tag{28}$$

here the integration $\int dV$ being carried out over the plasma region, and V and S being the volume and the cross-sectional area of the plasma respectively. The both results agree well. For example, when we preset parameters $\lambda^2 = 2 \times 10^{-5}$, $\mu = 0.01$ and $B_0 = 0$, i.e., without the vertical field, we obtain a = 10.2 cm, $\beta_p = 0.79$, $\ell_i = 0.98$ and $\Delta_{num} = 1.8$ cm from numerical computation and $\Delta_{cal} = 1.9$ cm from Eq.(28). The plasma current distribution resembles that expressed by a parabolic function. The linear dependence of the displacement Δ_{num} of the plasma column on the vertical magnetic field is shown in Fig.2.

B) Square

Two examples are presented in Figs.3 and 4 for the cases with and without a vertical field respectively. The equi-flux surfaces are almost circular near the magnetic axis.

C) Rectangle (belt pinch).

The vertical length of the shell cross-section is elongated, for example, 3 times the horizontal length as shown in Fig.5. In Fig.5a it is shown that the vacuum region is rather wide at the upper and lower sides of the plasma and the magnetic surface becomes elliptic. Figures 5b and 5c are the examples which correspond to the 'doublet' and 'triplet' configuration respectively. These multi= connected configurations are obtained by making the parameters λ^2 large. This aspect is similar to the wave phenomenon in a cavity to which the Helmholtz equation $\Delta\psi + k^2\psi = 0$ can be applied. The appearance of multi-connected configurations with large λ^2 corresponds to the appearance of waves of higher modes with large k^2 which is the wave number of the excited wave.

D) Finger Ring Type

The cross-section of the shell is chosen as expressed by a function

$$(60^2 - R^2 - 4Z^2/3)(R - 30) = 0. \qquad (29)$$

In this case, in spite of the deformed cross-section of the shell, the magnetic surface is almost elliptic as shown in Fig.6a for the plasma parameters $\beta_p \sim 1$ and $q \sim 1$. This result suggests that a certain external control field may be necessary in order to make the plasma cross-section

resemble the shape of the shell. A doublet type configuration is also obtained (Fig.6b).

E) A Ring Coil Placed inside the Shell

A ring coil is placed inside the square shell. A 'virtual limiter' is placed at $R \leq 39$ cm. A tear drop type configuration is obtained as shown in Fig.7. The same procedure can be available to obtain the equilibrium configurations in the cases with the open shell and without the shell, for example for DIVA [13] and Multipole Tokomak [6].

IV. Conclusion

We have shown a method to obtain the plasma configuration inside the shells of various shapes for various β_p and q. This method is applicable to the cases with arbitrary control fields which are produced by the currents flowing in axisymmetric coils (ring coils). It does not matter whether the coils are located inside the shell or not, and whether the control fields are steady or pulsive. Therefore, we can apply this method to find the magnetic configuration for shell-less devices. In this case we suppose a shell which is placed far from the region occupied by the plasma and the control field coils so that the effect of the current induced in the shell on the mag-

netic configuration is small. The function $S(\psi)$, which defines the region where the plasma current can flow, is convenient to treat with the equilibrium problem by the numerical method.

Although we have decribed the numerical method for a paticular plasma current distibution in this paper, this method can be applied for different plasma current distributions, for example, for the flat distribution, as far as the current sheet on the plasma surface is absent.

The author is grateful to Dr. M. Masuzaki and the colleagues for several helpful dicussions and to Dr. T. Watanabe for his allowance to use his program for drawing the equi-flux surfaces.

Appendix

The Method of Computation

To solve Eq.(8) for a rectangular shell, we try, at first, to use the standard alternating direction implicit method with the following iteration scheme

$$\{-L_R - f(R)S(\psi_n) + \rho\}\psi_{n+1/2} = (L_Z + \rho)\psi_n, \qquad (A\text{-}1)$$

and

$$\{-L_Z - f(R)S(\psi_{n+1/2}) + \rho\}\psi_{n+1} = (L_R + \rho)\psi_{n+1/2}, \qquad (A\text{-}2)$$

where ρ is an implicit parameter, L_R and L_Z are $R\frac{\partial}{\partial R}\frac{1}{R}\frac{\partial}{\partial R}$ and $\frac{\partial^2}{\partial Z^2}$ respectively and $f(R) = \lambda^2R^2 + \mu$. If an error ε_n is present at the n-th step, that is , if $\psi_n = \bar{\psi} + \varepsilon_n$ where $\bar{\psi}$ is a solution of Eq.(8), equations for ε_n become, up to order of ε,

$$\{-L_R - f(R)S(\bar{\psi}) + \rho\}\varepsilon_{n+1/2} = (L_Z + \rho)\varepsilon_n , \qquad (A\text{-}3)$$

and

$$\{-L_Z - f(R)S(\bar{\psi}) + \rho\}\varepsilon_{n+1} = (L_R + \rho)\varepsilon_{n+1/2} . \qquad (A\text{-}4)$$

Here we have used relations that $S(\psi_n) = S(\bar{\psi}) + \varepsilon_n\delta(\bar{\psi})$ and $\psi\delta(\psi) \equiv 0$, and we have neglected the terms of $\varepsilon_n\varepsilon_{n+1/2}\delta(\psi)$ as a higher order of ε. Now, we expand ε_n with eigen-functions $\chi_{1,r}(R)$ and $\chi_{2,s}(Z)$ of the differential operator L_R and L_Z, i.e. $-L_R\chi_{1,r} = a_r\chi_{1,r}$ and $-L_Z\chi_{2,s} = b_s\chi_{2,s}$;

$$\varepsilon_n = \sum_{r,s} A^n_{r,s} \chi_{1,r}(R) \chi_{2,s}(Z). \qquad \text{(A-5)}$$

Putting Eq. (A-5) into Eq. (A-3), we find

$$\sum_{r,s} A^{n+1/2}_{r,s} (a_r - f(R)S(\bar{\psi}) + \rho) \chi_{1,r} \chi_{2,s} \qquad \text{(A-6)}$$

$$= \sum_{r,s} (-b_s + \rho) A^n_{r,s} \chi_{1,r} \chi_{2,s}.$$

Using the orthogonality of $\chi_{1,r}$ and $\chi_{2,s}$, we have

$$(a_r + \rho) A^{n+1/2}_{r',s'} - \sum_{r,s} A^{n+1/2}_{r,s} F_{r',s',r,s} = (-b_s + \rho) A^n_{r',s'}, \qquad \text{(A-7)}$$

where $$F_{r',s',r,s} = \int f(R) S(\bar{\psi}) \chi_{1,r} \chi_{1,r'} \chi_{2,s} \chi_{2,s'} r(R) dR dZ$$

and $r(R)$ is a weight function. As rigorous mathematical analysis is not of our interest, we roughly estimate $F_{r',s',r,s}$ as follows,

$$F_{r',s',r,s} \sim 0, \text{ when } r \neq r' \text{ and } s \neq s' \qquad \text{(A-8)}$$

and

$$0 \leq F_{r',s',r',s'} \equiv F_{r',s'} \leq F, \qquad \text{(A-9)}$$

where F is a maximum value of $F_{r',s'}$ for all values of r' and s'. Then from Eq. (A-7) we have

$$A^{n+1/2}_{r',s'} = \frac{-b_{s'} + \rho}{a_{r'} + \rho - F_{r',s'}} A^{n}_{r',s'} \qquad \text{(A-10)}$$

From Eq.(A-4), with the same calculation, we have

$$A^{n+1}_{r',s'} = \frac{-a_{r'} + \rho}{b_{s'} + \rho - F_{r's'}} A^{n+1/2}_{r',s'} \ . \qquad \text{(A-11)}$$

Therefore, we have the following relation,

$$A^{n+1}_{r,s} = E_{r,s} A^{n}_{r,s} \ , \qquad \text{(A-12)}$$

where $E_{r,s} = \frac{-a_r + \rho}{a_r + \rho - F_{r,s}} \cdot \frac{-b_s + \rho}{b_s + \rho - F_{r,s}}$.

If the absolute value $|E_{r,s}|$ is less than the unity for all values of r and s, the convergence of this iteration scheme is satisfied. However, any value of ρ can not satisfy the above condition for the allowed range of a_r, b_s and $F_{r,s}$ ($0 < a_r, b_s < \infty$ and the range of $F_{r,s}$ is written in Eq.(A-9)). When $\rho > F$, we find following relations,

$$-1 < \frac{-a_r + \rho}{a_r + \rho - F_{r,s}} < \frac{\rho}{\rho - F}, \qquad \text{(A-13)}$$

and also

$$-1 < \frac{-b_s + \rho}{b_s + \rho - F_{r,s}} < \frac{\rho}{\rho - F}, \qquad \text{(A-14)}$$

where $\rho/(\rho - F)$ is larger than the unity. Then, we find the range of $E_{r,s}$,

$$-\frac{\rho}{\rho - F} < E_{r,s} < \left(\frac{\rho}{\rho - F}\right)^2. \qquad \text{(A-15)}$$

When $\rho < F$, $E_{r,s}$ increases infinitely as $a_r \to F_{r,s} - \rho$.

In order to let the convergent limit lie within the unit circle, the method developed by Marder and Weitzner is used. We denote the one cycle of the iteration steps written in Eqs.(A-1) and (A-2) by

$$L\psi_{n+1/3} + S(\psi_n)f(R)\psi_n = 0. \qquad \text{(A-16)}$$

And we consider the following iteration,

$$L\psi_{n+1/3} + S(\psi_n)f(R)\psi_n = 0, \qquad \text{(A-17)}$$

$$L\psi_{n+2/3} + S(\psi_{n+1/3})f(R)\psi_{n+1/3} = 0, \qquad \text{(A-18)}$$

and

$$\psi_{n+1} = (1 - G)\psi_n + 2G\psi_{n+1/3} - G\psi_{n+2/3}, \qquad \text{(A-19)}$$

where G is a positive constant. Then, applying the calculations from (A-3) to (A-12) to each step from (A-17) and (A-18), we have the following relation,

$$A_{r,s}^{n+1} = \{1 - G(1 - E_{r,s})^2\}A_{r,s}^{n}. \qquad \text{(A-20)}$$

For convergence of this iteration scheme it is necessary that $|1 - G(1 - E_{e,s})^2| < 1$. Then using (A-15), the conver-

gence condition is represented by the following inequalities,

$$1 - \sqrt{\frac{2}{G}} < -\frac{\rho}{\rho - F} \qquad \text{(A-21)}$$

and

$$1 + \sqrt{\frac{2}{G}} > \left(\frac{\rho}{\rho - F}\right)^2 . \qquad \text{(A-22)}$$

When we select ρ which is satisfactorily larger than F, the convergence condition is satisfied when $0 < G < 1/2$. In practical computation, we have selected $G = 0.45$ and $\rho = (3 \sim 4) f(R_{max})$.

References

[1] Ohkawa, T., Kakuyugo-Kenkyu 20 (1968) 557.

[2] Coppi, B., Dagazian, R. and Gajewski, R., Phys. Fluids 15 (1972) 2405.

[3] Zwicker, H. and Wilhelm, R., Proc. of Fifth European Conf. Controlled Fusion and Plasma Physics (Grenoble, 1972) vol.II 59.

[4] Furth, H. P. and Yoshikawa, S., Phys. Fluids 13 (1970) 2573.

[5] Artsimovich, L. A. and Shafranov, V. D., JETP. Lett. 15 (1972) 51.

[6] Feneberg, W. and Lackner, K., Nuclear Fusion 13 (1973) 549.

[7] Shafranov, V. D., Review of Plasma Physics, edited by Leontovich, M. A. (Consultants Bureau, New York, 1966), vol.2.

[8] Suzuki, Y., Nuclear Fusion 13 (1973) 369.

[9] Suzuki, Y., IPPJ-159 (Research Report of Institute of Plasma Physics, Japan).

[10] Marder, B. and Weitzner, H., Plasma Physics 12 (1970) 435.

[11] Yoshikawa, S., Phys. Fluids 15 (1972) 1683.

[12] Callen, J. D. and Dory, R. A., Phys. Fluids 15 (1972) 1532.

[13] Kitsunezaki, A., Maeda, H., Shimomura, Y. and Yoshikawa, M., 3rd International Conference on Toroidal Plasma Confinement (1973) paper G2.

Figure Captions

Fig.1. A typical equilibrium configuration in a circular shell. $\lambda^2 = 2 \times 10^{-5}$, $\mu = 0.01$, ($q = 1.72$, $\beta_p = 0.78$, and $M = 0.01$).

Fig.2. The effect of the vertical field on the center of the plasma surface. The solid line means the displacement given by the analytical results ($\beta_p = 0.95$, $\ell_i = 1$). The vertical field is expressed by $\psi_e = -cR^2$.

Fig.3. Equi-flux surfaces in a right rectangular shell. The vertical magnetic control field is not applied. $\lambda^2 = 2 \times 10^{-5}$, $\mu = 0.01$, $M = 0.001$, ($q = 5.7$, $\beta_p = 0.81$).

Fig.4. Equi-flux surfaces in the right rectangular shell. A vertical magnetic control field is applied. $\lambda^2 = 2 \times 10^{-5}$, $\mu = 0.01$, $M = 0.001$, ($q = 6.6$, $\beta_p = 0.79$).

Fig.5. Elongated rectangular shell and magnetic surfaces.

a) 'singlet' $\lambda^2 = 1 \times 10^{-5}$ $\mu = 0.001$

b) 'doublet' $\lambda^2 = 1.2 \times 10^{-5}$ $\mu = 0.001$

c) 'triplet' $\lambda^2 = 3.6 \times 10^{-5}$ $\mu = 0.001$

Fig.6. A shell of finger ring type of the shell.

a) 'singlet' $\lambda^2 = 2 \times 10^{-5}$ $\mu = 0.001$

b) 'doublet' $\lambda^2 = 3.6 \times 10^{-5}$ $\mu = 0.001$

Fig.7. Right rectangular shell with a ring coil located inside it (tear drop type). A virtual limiter is placed at the left hand of the broken line. $\lambda^2 = 1.4 \times 10^{-4}$, $\mu = -0.5$.

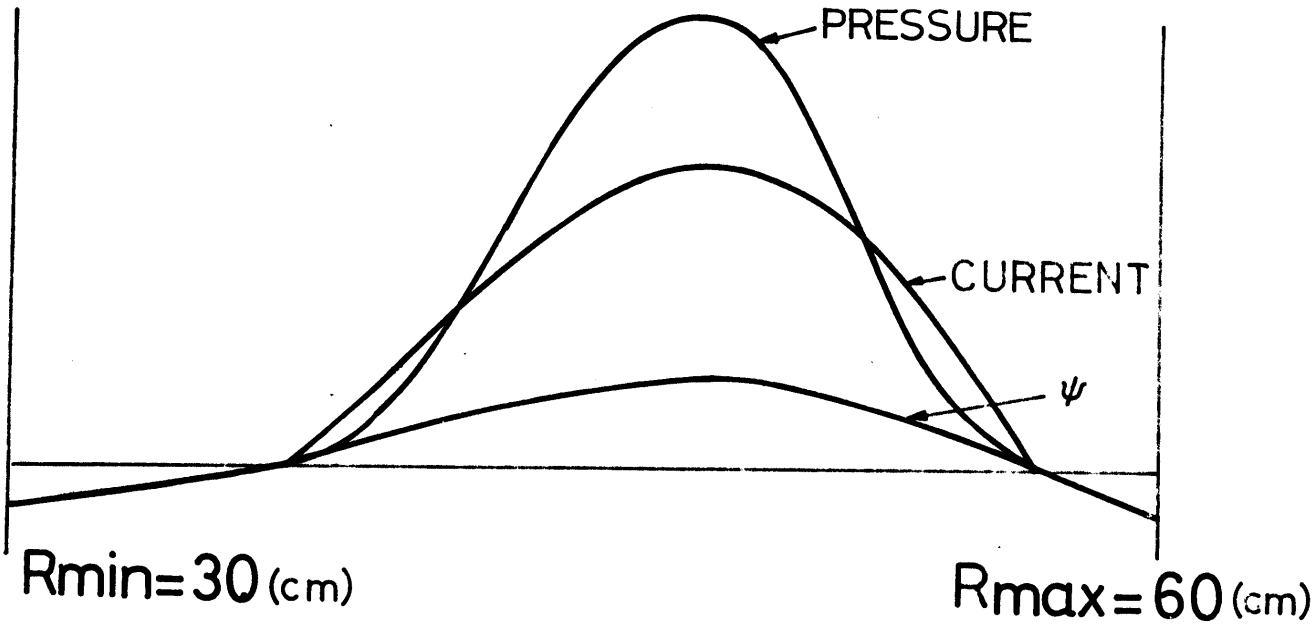

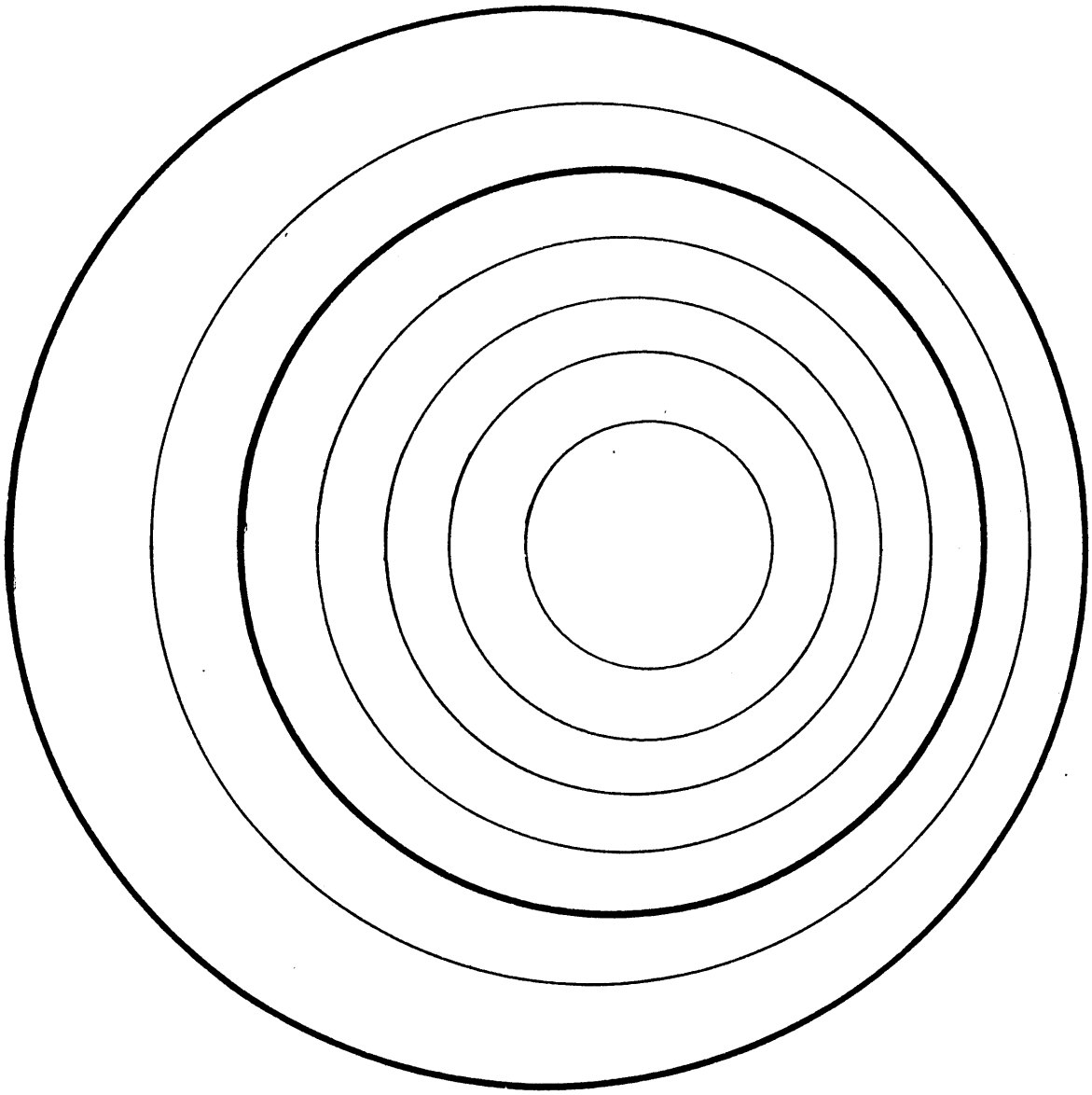

Fig. 1.

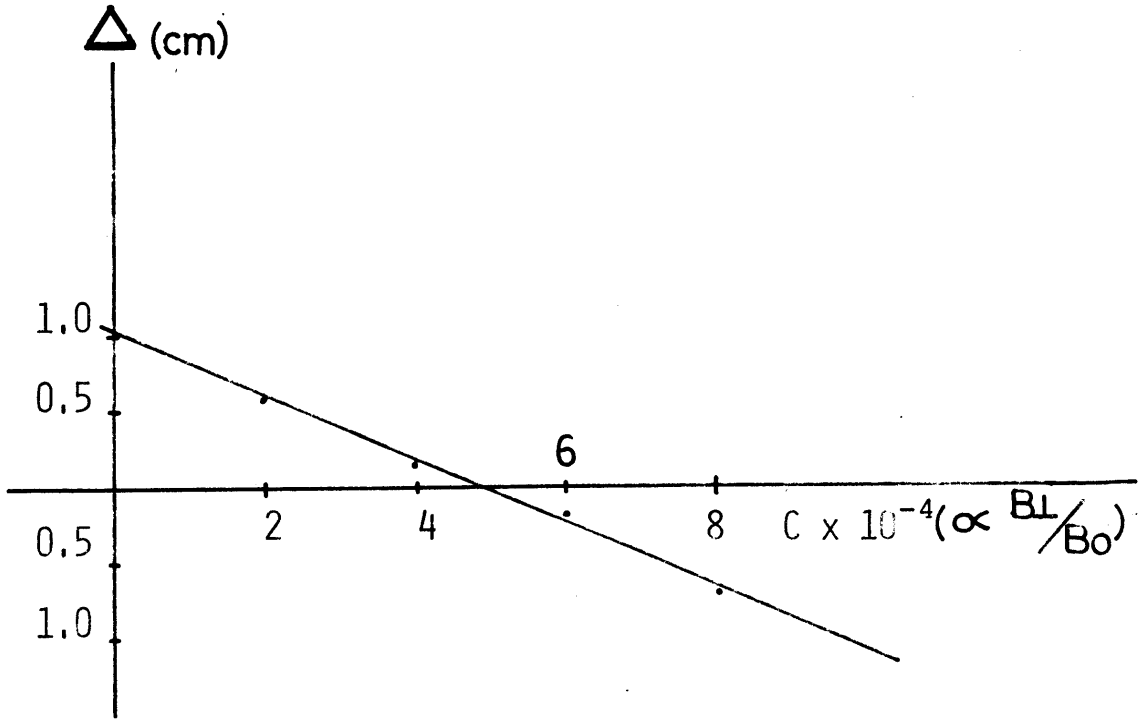

Fig. 2.

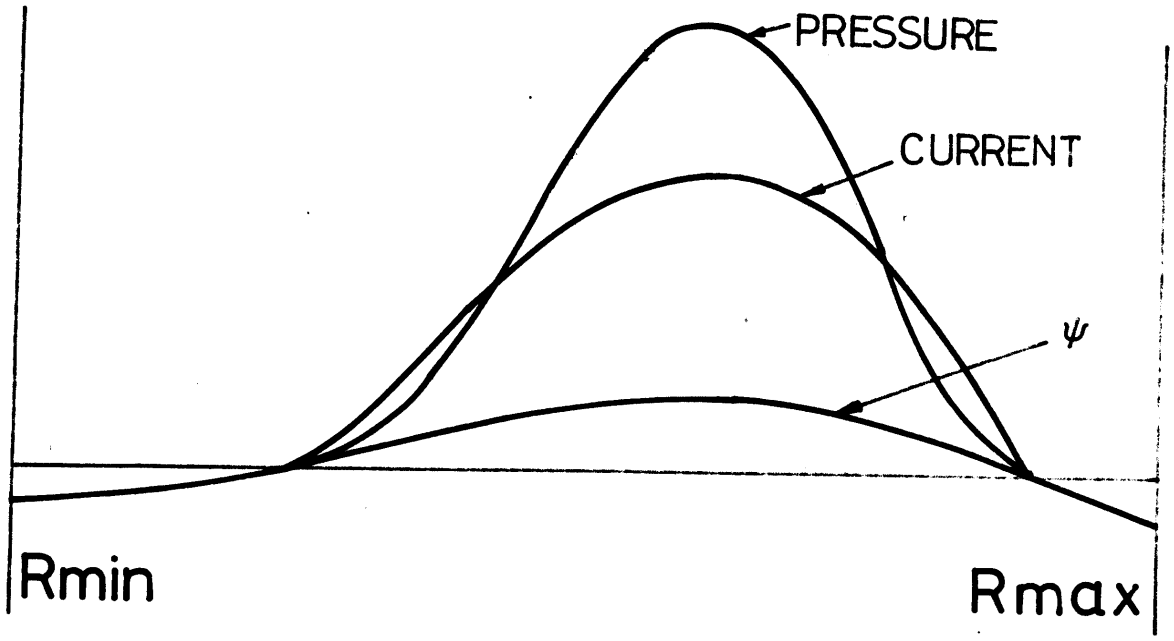

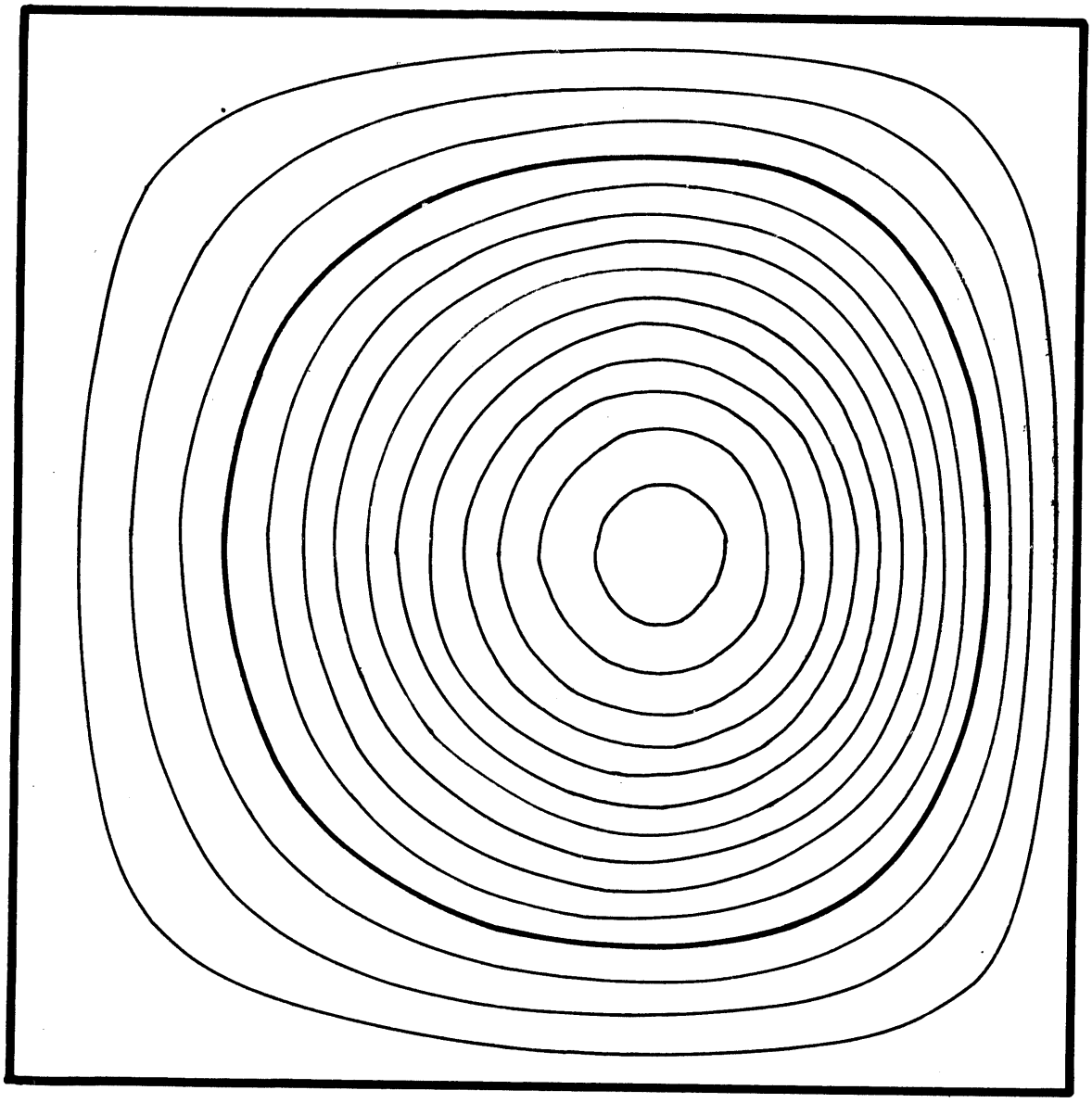

Fig. 3.

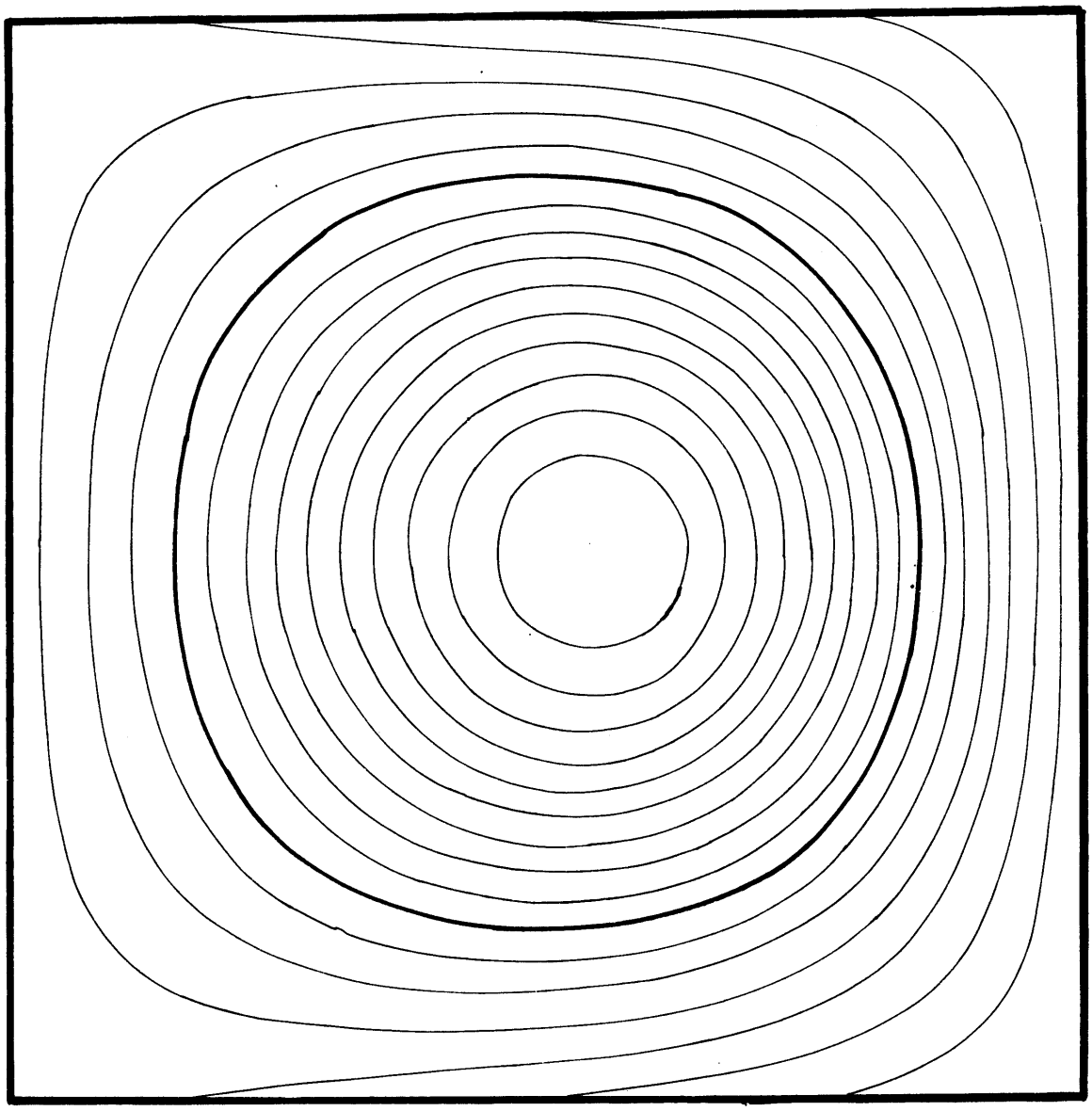

Fig. 4.

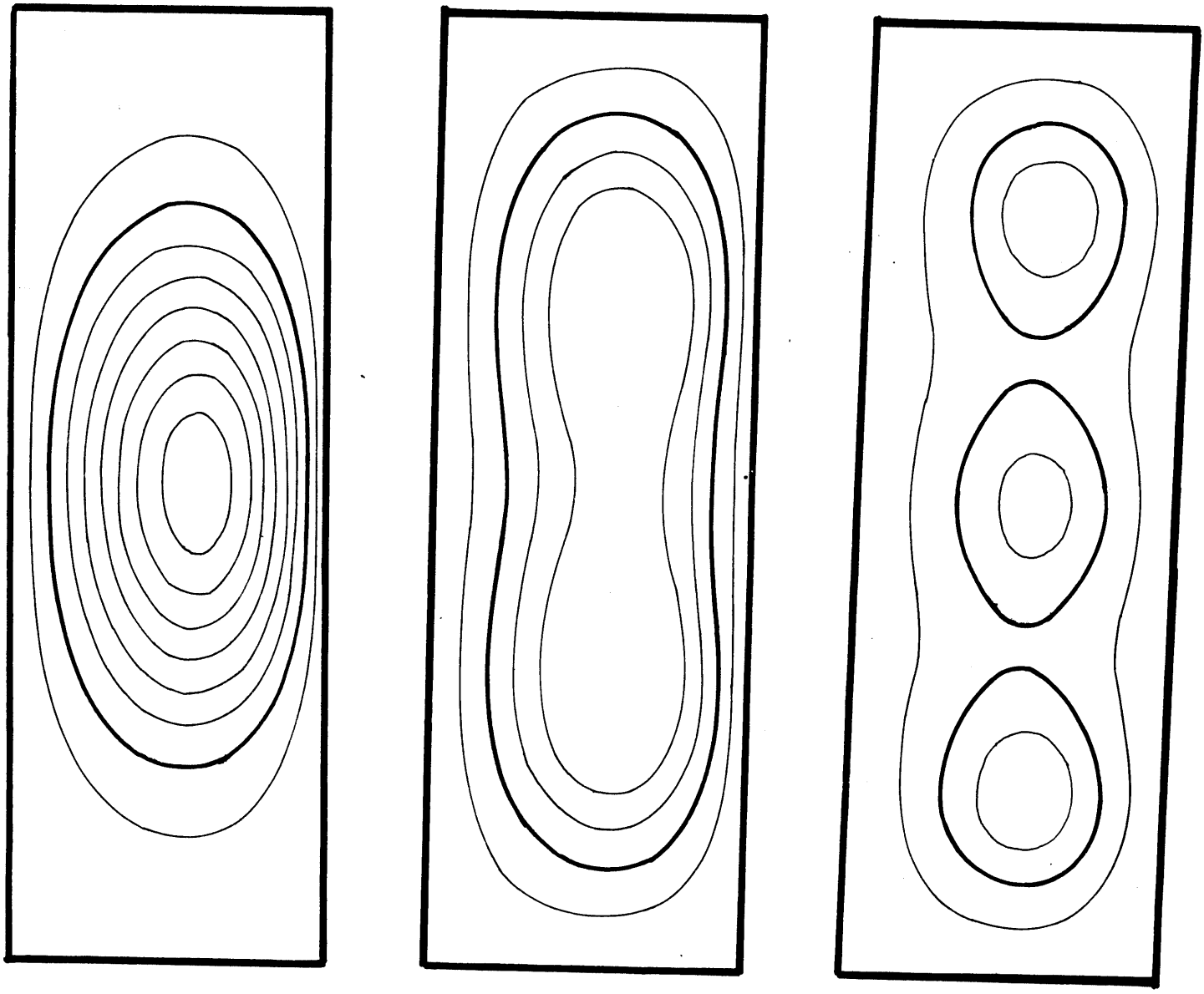

(a) (b) (c)

Fig. 5.

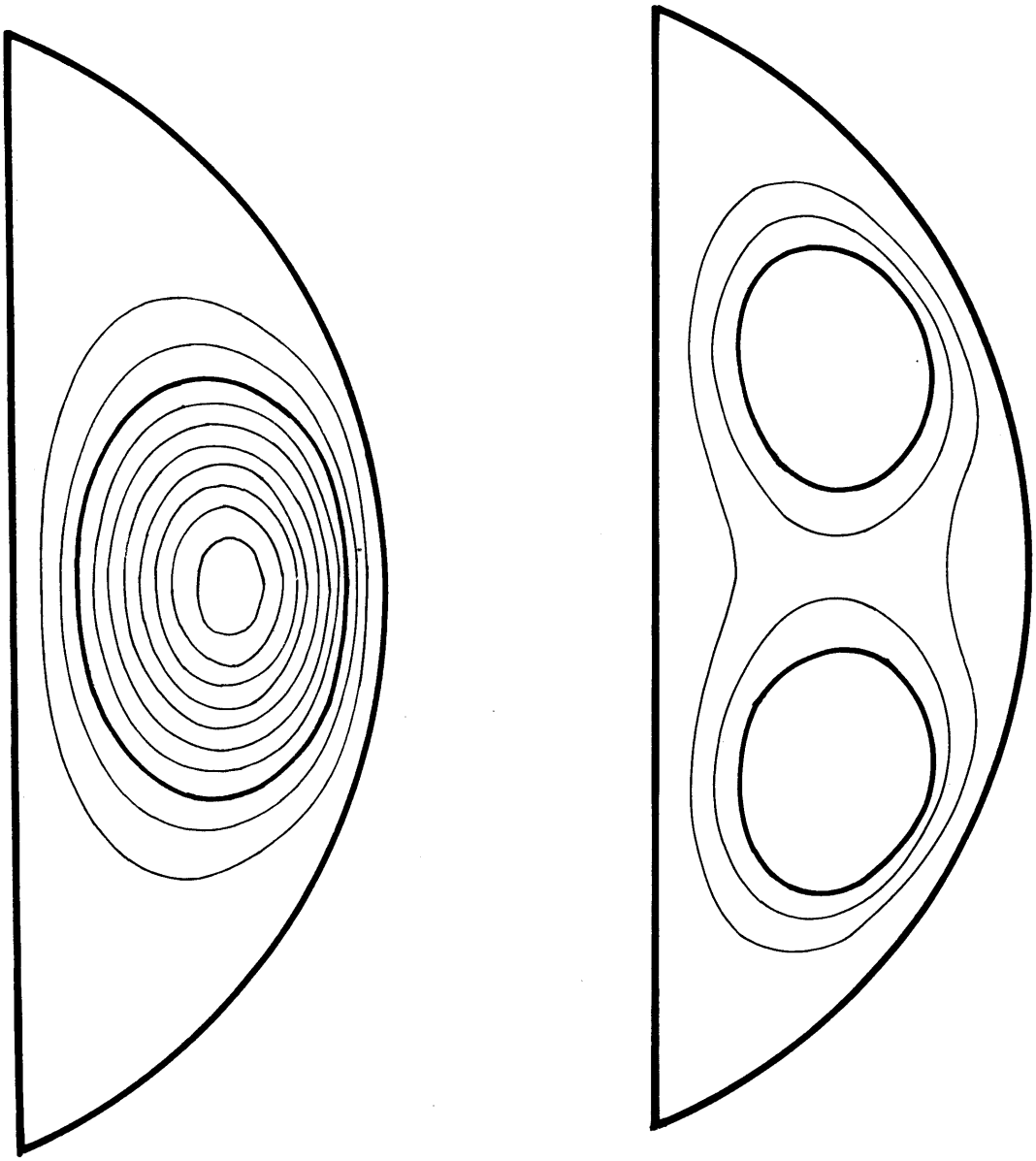

(a) (b)

Fig. 6.

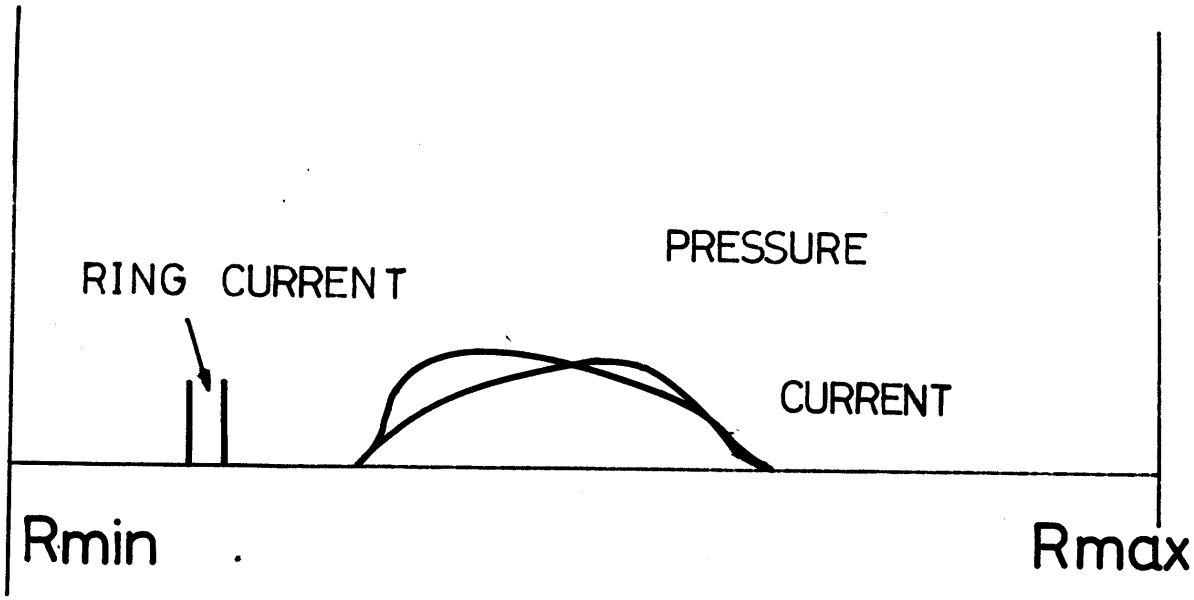

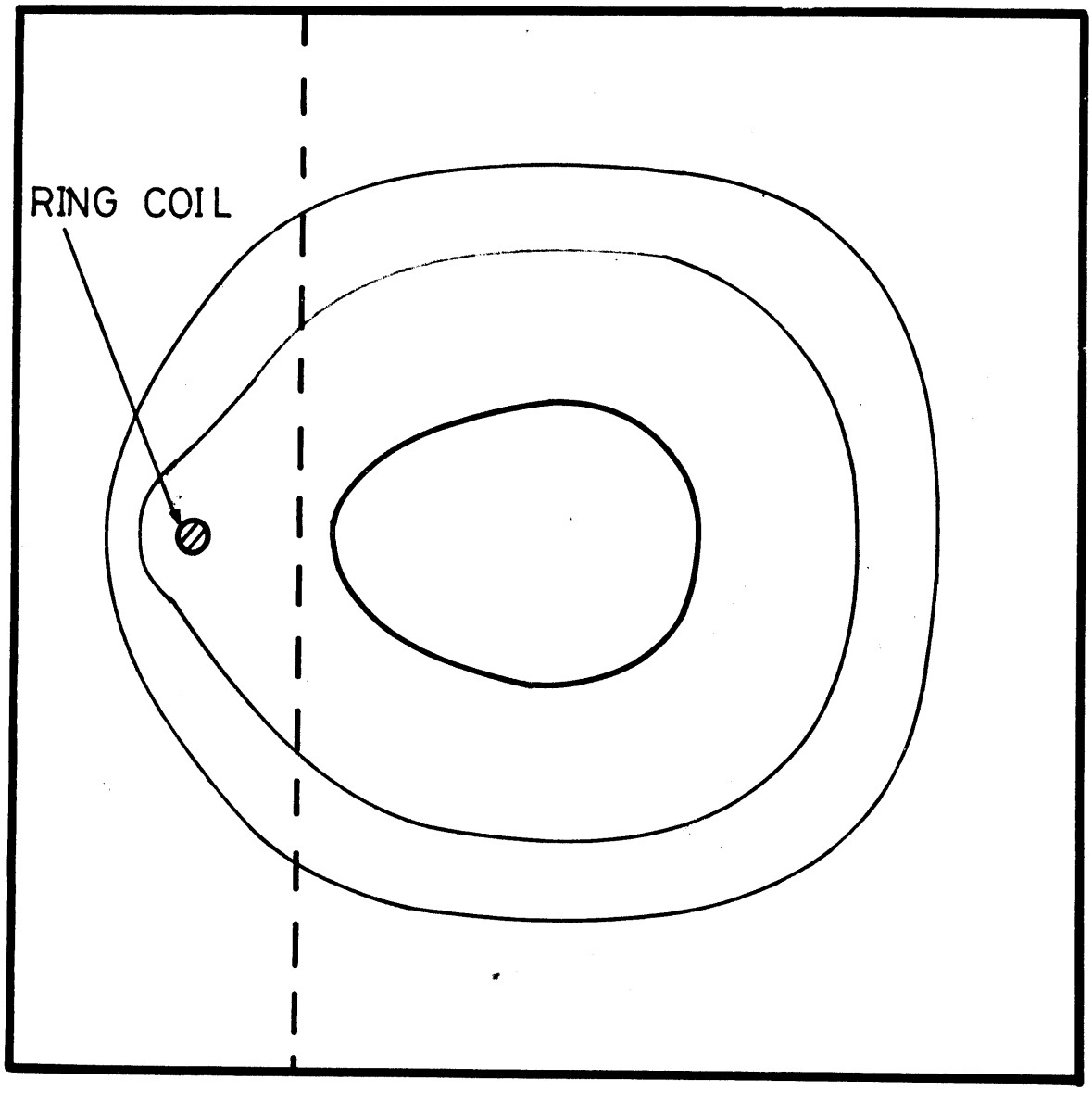

Fig. 7.